Comorbidity-Shaped Cell States in Alzheimer's Disease: Single-Nucleus Dissection of Nine Comorbidities in the Aged Human Prefrontal Cortex

Tristan Sun

Under the direction of
Professor Manolis Kellis
Computer Science and Artificial Intelligence Laboratory
Massachusetts Institute of Technology

Research Science Institute
August 4, 2026

Abstract

Comorbidities are an important yet understudied aspect of Alzheimer's disease etiology. We analyzed paired single-nucleus RNA sequencing and clinical history data from 427 donors to characterize the transcriptional effects of nine comorbidities. Because human cohorts exhibit significant heterogeneity, we applied the cell-projected phenotypes method [1] to identify donors whose transcriptional states were concordant with their clinical diagnosis. All pairs of comorbidities except hypertension and smoking showed significantly different cell-type-specific differentially expressed gene burden profiles ($p_{\text{adj}} < .05$). Transcriptional responses separated by phenotype into two classes characterized by bioenergetic state. Among the comorbidities examined, thyroid disease elicited the most AD-like response. By characterizing the transcriptional heterogeneity of AD comorbidities, this work provides a foundation for the development of personalized AD preventions and treatments.

Summary

Alzheimer's disease (AD), the most common cause of dementia worldwide, affects every individual differently. Because most AD patients are elderly, many suffer from other comorbid chronic health conditions. Previous studies have shown that these comorbid diseases and lifestyle factors increase the risk for and accelerate the progression of AD. However, although this association is well-established, the molecular mechanisms through which comorbidities alter AD progression remain poorly understood. We analyzed nine comorbidities in a dataset with 427 donors, finding that comorbidities separate into two major classes that differ on a molecular level. Our work provides a foundation for personalized AD therapeutic based on comorbidity history.

1 Introduction

1.1 Alzheimer's disease is an escalating health crisis

Alzheimer's disease (AD) is the leading cause of dementia worldwide, accounting for 60% to 80% of all cases [2]. More than 7 million Americans have AD, and this number is expected to double by 2060 as the population ages [3]. While advances in prevention and treatment reduced mortality from other major diseases including stroke, heart disease, and HIV from 2000 to 2022, deaths attributed to AD increased by 142.4% over the same period [2].

Despite decades of extensive intellectual and financial investment [4], AD clinical trials have historically exhibited high failure rates [5]. Although new drugs such as the anti-amyloid monoclonal antibodies lecanemab [6] and donanemab [7] have generated significant optimism, their marginal effectiveness and adverse effects remain major obstacles [8]. While these treatments moderately slow cognitive decline by reducing markers of amyloid in patients with early AD, they are incapable of stopping cognitive decline or restoring lost cognitive function [6, 7].

Heterogeneity is one factor that complicates the treatment of AD. Because AD and other age-related dementias predominantly affect older adults, more than 86% of people with dementia also have at least two other chronic health conditions [9]. These comorbid conditions contribute to diverse manifestations of AD; patients with the same clinical diagnosis of AD have been shown to activate different molecular programs [10]. However, state of the art amyloid-removing drugs ignore AD's inherent heterogeneity and treat the disease as a single monolithic disorder rather than a condition which manifests differently in every patient. The limited efficacy of these one-size-fits-all treatments suggests that personalized strategies are needed that account for this heterogeneity, including therapeutics informed by a patient's history of comorbidities.

1.2 Comorbidities control a large and modifiable share of AD risk

In addition to contributing to the heterogeneity of AD [10], many comorbidities are also known to increase the risk of AD. For example, the 1999 Rotterdam Study examined 6,370 elderly patients and found that type 2 diabetes almost doubled the risk of dementia, especially among patients treated with insulin [11]. Another epidemiological study conducted among Catholic nuns, priests, and brothers in 2004 revealed that type 2 diabetes increased the risk of AD by 65% [12], corroborating the findings of the 1999 Rotterdam Study.

Hypertension is another comorbidity which increases AD risk. An analysis of 8639 individuals from the 1991 Whitehall II study [13] found that midlife systolic blood pressure above 130 mmHg is associated with increased dementia risk irrespective of cardiovascular disease [14]. Similarly, midlife obesity [15, 16], head injury [17], thyroid dysfunction [18], alcohol use disorder [19] and smoking [20] have all been associated with an increased risk of AD, while Parkinson's disease has been associated with a substantially increased risk of dementia [21].

The 2020 *Lancet* Commission attributed approximately 40% of dementia risk to 12 modifiable risk factors [22]. Elucidating how comorbidities affect cortical transcriptional state would therefore serve two complementary goals. First, this knowledge would allow us to better characterize the heterogeneity of AD, allowing the development of personalized AD treatments. Second, identifying the mechanisms through which comorbidities predispose for AD could reveal targets for interventions to prevent the disease.

1.3 Characterizing the molecular mechanisms of comorbidities

Although the epidemiological link between comorbidities and AD risk is well-established, the biological pathways underlying these relationships remain poorly understood. In particular, it remains largely unknown which types of brain cells are most affected by each comorbidity, which molecular pathways mediate the pathological effects of comorbidities, and whether clinically distinct conditions actually converge on similar underlying pathways.

To address these questions and thereby map the landscape of AD heterogeneity, we

conduct the first single-cell analysis of transcriptional changes in brain cells across a panel of comorbidities. This work enhances our understanding of AD etiology and lays the foundation for personalized methods which prevent or treat AD.

2 Methods

2.1 Single-nucleus profiling of ROSMAP donors

The Religious Orders Study (ROS) and the Rush Memory and Aging Project (MAP), together ROSMAP, are aging and dementia cohorts which combine longitudinal clinical data with detailed postmortem histological analysis [23]. Recently, single-cell RNA sequencing (scRNA-seq) and single-nucleus RNA sequencing (snRNA-seq) have made it possible to profile gene expression at the resolution of individual cells [24]. Although scRNA-seq provides more comprehensive transcriptional data than snRNA-seq by capturing both nuclear and cytoplasmic RNA transcripts, scRNA-seq is infeasible for neuronal cells due to their complex morphologies including extensive dendrites and axons. Furthermore, ROSMAP tissue samples are frozen after death [23], making it impossible to extract intact cells necessary for scRNA-seq. Therefore, we used snRNA-seq, which is the standard for single cell resolution profiling of the brain transcriptome because it does not suffer from the same limitations [25].

Previous work from the Kellis lab generated an snRNA-seq atlas of the aged human dorsolateral prefrontal cortex, covering 427 ROSMAP individuals balanced across cohort, sex, and AD status [26]. This massive-scale snRNA-seq profiling provides an unparalleled resource linking phenotypic characteristics to molecular programs.

All clinical and pathological data was obtained from the Rush Alzheimer's Disease Center Research Resource Sharing Hub (https://www.radc.rush.edu/home.htm) under an approved data use certificate. We analyzed the nine comorbidities summarized in Table 1. These comorbidities were selected because they are common in older adults, have been associated with elevated AD risk, and are sufficiently represented in the ROSMAP dataset to have

enough power for statistical analysis. Each comorbidity was collapsed to a boolean value of 0 or 1 except for body mass index, which was kept continuous as a z-score relative to the 427 other ROSMAP donors.

Table 1: Clinical phenotypes included in the analysis.

Comorbidity	ROSMAP variable	Encoding
Alzheimer's disease	`ADDiag2types`	Non-AD vs AD
Alcohol use	`ldai_bl`	< 1 vs ≥ 1 drink per month
Body mass index	`bmi_lv`	Continuous z-score
Diabetes	`diabetes_sr_rx`	Absent vs present
Head injury	`headinjrloc_bl`	No vs history with loss of consciousness
Heart disease	`heart_bl`	Absent vs present
Hypertension	`hypertension_bl`	Absent vs present
Parkinson's disease	`dxpark`	Absent vs present
Smoking	`smoking_bl`	Never vs former/current
Thyroid disease	`thyroid_bl`	Absent vs present

2.2 Cell-projected phenotype (CPP) derived subgrouping augments detection of differentially expressed genes (DEGs)

Stratification based solely on donor-level measurements dilutes comorbidity-associated signal because donors with the same phenotypic diagnosis possess heterogeneous molecular programs. To address this, we focus on donors whose transcriptional state is concordant with their phenotypic diagnosis following the CPP-derived subgrouping method developed in [1]. Briefly, CPP reveals intra-donor transcriptional heterogeneity by projecting donor-level phenotypes onto individual cells, assigning each cell a numerical score quantifying how phenotype-like its transcriptional state is. To accomplish this, we subsampled individuals with extreme cell counts, selected 2000 variable genes, retained the first 12 principal components in Seurat (v5.5.1), and built a $k = 30$ nearest-neighbor graph. Cells were assigned to (possibly overlapping) neighborhoods by running the Milo sampling algorithm (miloR v2.6.0) on this graph. Cell scores were computed based on both proximity to neighborhoods and phenotypic enrichment of cell donors in those neighborhoods (CellProjectedPhenotypes v1.0.0).

Out of 54 high-resolution cell types annotated by [26], Fib SLC4A4 and Mic MKI67

were present in fewer than 150 total donors and were thus excluded. 4 non-AD donors with fewer than 15 high-resolution cell types were excluded. For each of 218 remaining non-AD donors, these scores were aggregated for each of 52 remaining high-resolution cell types and missing values were imputed with the R package eimpute (v0.2.4). Based on these 52 aggregated scores calculated per donor, we clustered donors into three groups (CPP-low, CPP-intermediate, CPP-high) using the k-means algorithm with $k = 3$. The clustering was robust because 30 seeds agreed at adjusted Rand index ≥ 0.992. Differentially expressed gene (DEG) analysis was performed between CPP-high, phenotype-positive donors vs CPP-low, phenotype-negative donors using DESeq2 (v1.50.2), with age, batch, post-mortem interval, sex and years of education as covariates. Genes without an approved symbol from the HUGO Gene Nomenclature Committee and genes with fewer than 10 total counts were excluded. Donors with fewer than 10 nuclei were excluded. We used the Benjamini–Hochberg adjusted p-value for all downstream analyses. We call a gene differentially expressed if $p_{\text{adj}} < 0.05$, $|\log_2 \text{FC}| > 0.5$, and it is expressed in at least 10% of cells. Panels **(A)**, **(B)** and **(C)** of Figure 1 show that CPP-based subgrouping of donors results in the detection of significantly more DEGs.

For all phenotypes besides AD, we restricted differential expression analyses to only non-AD donors (222 out of 427) for three reasons. First, because the transcriptional effect of AD is very strong compared to other clinical phenotypes, comparing donors spanning diverse stages of AD pathology could have masked transcriptional signatures of interest. Second, because neuroinflammation, astrogliosis and other pathological effects of AD alter the transcriptome in ways that could potentially hide or exacerbate the signatures of other phenotypes, we analyzed only non-AD donors to ensure a consistent baseline of low AD-associated transcriptional change. Third, in late-stage AD donors, physiological measures (i.e. blood pressure, presence of infarcts, body mass index) can be effects of AD rather than factors which lead to AD. Therefore, we did not include late-stage AD donors because doing so may have caused us to find circular, spurious similarities between the molecular signature

of AD and other phenotypes.

For AD, we performed an identical DEG analysis using all 427 donors rather than only the 222 non-AD donors. Panels **(D)**, **(E)** and **(F)** of Figure 1 show that CPP-based subgrouping of donors significantly increases the detection of AD DEGs.

2.3 DEG response vectors elucidate similarities in transcriptional effects of clinically distinct phenotypes

To characterize the similarities between transcriptional responses from distinct phenotypes, we represented responses as vectors of $\log_2$ FCs for genes in the union of DEGs over all (phenotype, cell type) pairs. Although genes were required to be expressed in at least 10% of cells to be considered differentially expressed, each entry in the high-dimensional response vector represented the raw $\log_2$ FC with no filter based on percent expression. To prevent outlier genes from dominating, we clipped $\log_2$ FC values at the 99.9th percentile (numerical value: 2.18). We define the distance between two response vectors as one minus their Pearson correlation. To visualize responses, we generated t-SNE embeddings, as shown in panels **(A)** and **(B)** of Figure 3. Responses were clustered into two classes by running the k-means algorithm with $k = 2$ on the high-dimensional response vectors. Responses which generated fewer than 10 DEGs were excluded from embedding and clustering because they contained insufficient differential expression signal.

2.4 Functional enrichment analysis

For each of the upregulated and downregulated gene sets, genes were sorted by their DESeq2 Wald statistic. Gene set enrichment analysis (GSEA) was performed with `fgseaMultilevel` [27, 28] using GOBP and KEGG. Enrichment was called at $p_{\text{adj}} < 0.05$. To better elucidate the functionality captured within the pathways, we manually selected representative terms based on pathway function and non-redundancy.

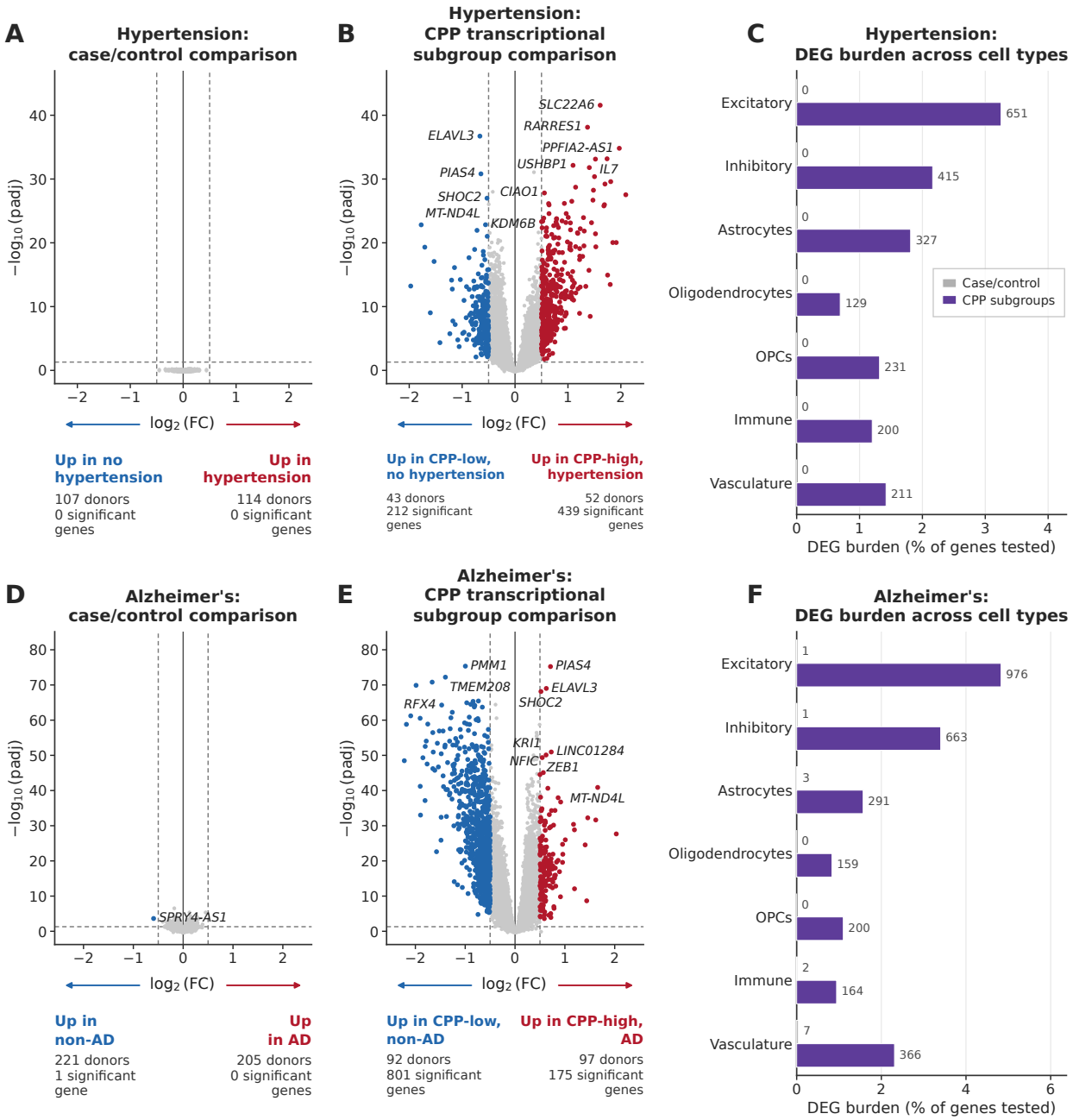

Figure 1: CPP-derived subgrouping augments detection of differentially expressed genes. **(A - C)** show hypertension DEGs detected by analyzing non-AD donors, while **(D - F)** show AD DEGs detected by analyzing all donors. **(A, D)** Donors split on clinical phenotype alone. **(B, E)** Donors split on the conjunction of CPP clustering and clinical phenotype.

3 Results and Discussion

3.1 Comorbidities alter transcriptional state in a cell-type-specific manner

We performed differential expression analysis for every (comorbidity, cell type) pair, as well as a reference analysis for Alzheimer's disease. DEG counts and donor counts are shown in Table 2. We calculated the DEG burden, defined as the number of DEGs divided by the number of genes tested, for each of the 70 comparisons. The DEG burden is a measure of the strength of a transcriptional response. DEG burden normalizes by the number of tested genes thereby accounting for differences in total number of genes. We found that, across phenotypes, burden was highly concentrated in neurons (Figure 2). However, several notable patterns emerged in non-neuronal cell types (Figure 2). Oligodendrocytes were the least responsive cell type on average. Hypertension elicited its highest non-neuronal DEG burden in astrocytes, followed by vasculature cells. Previous work has established that astrocytes undergo reactive astrogliosis under hypertensive conditions, potentially mediated by deterioriation of the blood-brain barrier [29, 30]. This could explain why the DEG burden due to hypertension is highest in astrocytes and vasculature cells. Diabetes was found to elicit its highest DEG burden in OPCs and oligodendrocytes, consistent with previous work which found that hyperglycemic conditions were associated with a decreased number and dysfunction of OPCs [31]. Alcohol consumption was associated with the highest DEG burden in astrocytes, matching previous findings that chronic ethanol consumption in adult mice produces astrocyte-specific transcriptomic responses related to calcium signaling and extracellular matrix regulation [32]. Moreover, alcohol consumption was also associated with high DEG burden in OPCs, consistent with the earlier finding that chronic alcohol consumption impairs myelin generation in the adult mouse brain, potentially through dysregulation of epigenetic processes regulating OPC differentiation [33]. Parkinson's disease was found to induce the highest DEG burden in OPCs but only an attenuated response in oligodendrocytes, an observation related to the

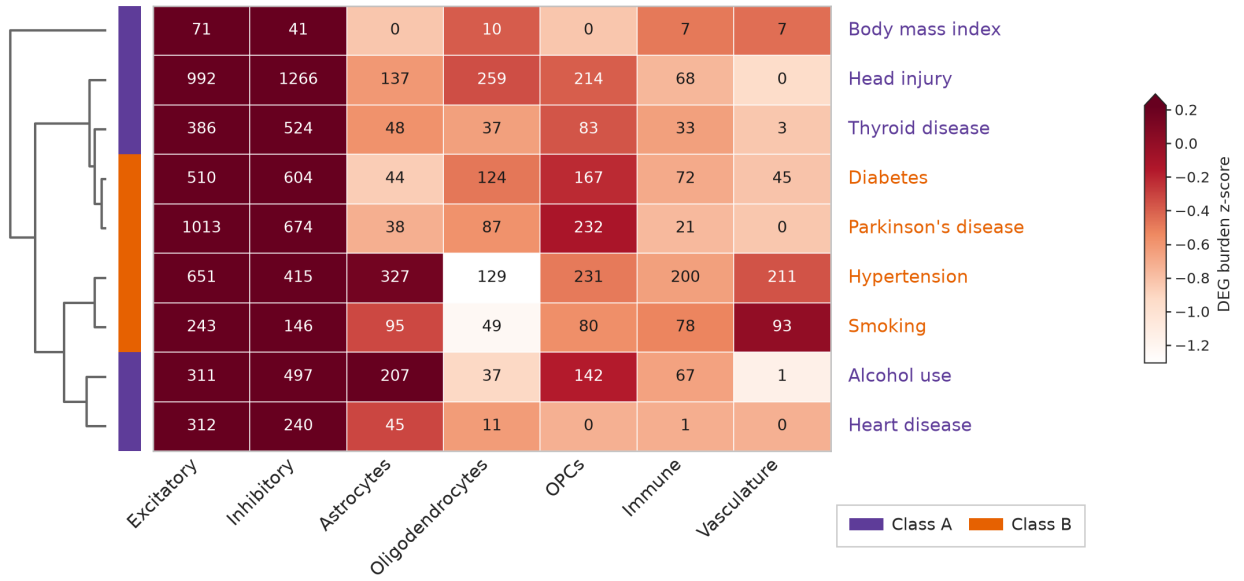

Figure 2: Different comorbidities elicit distinct cell-type-specific DEG burden patterns. Hierarchical clustering of comorbidities is performed based on the similarity of DEG burden patterns in non-neuronal cell types, quantified by Pearson correlation. Each cell's color represents the z-score of its DEG burden compared to the other DEG burdens in the same row, so colors are only comparable within the same row. Each cell's number represents the raw number of DEGs detected in its comparison.

findings of a previous study of the substantia nigra which found that OPC DEGs, but not oligodendrocyte DEGs, were associated with the severity of motor dysfunction [34].

Figure 2 suggests that each comorbidity elicits a distinct distribution of DEG burden across cell types. To verify the statistical significance of this observation, we fitted a binomial generalized linear model to the DEG burden across cell types. For each pair of comorbidities, we performed a likelihood-ratio test to determine whether the burden pattern differed. After Benjamini–Hochberg false discovery rate correction, all pairs except hypertension and smoking ($p_{\text{adj}} = 0.351$) were found to differ significantly at $p_{\text{adj}} < 0.05$.

3.2 Responses cluster first by phenotype into two classes and then by cell type

Applying k-means clustering with $k = 2$ to the 59 (condition, cell type) responses which produced at least ten DEGs, we identified two classes (Figure 3 panel A, silhouette score 0.452). Notably, class membership was unanimous within each condition. All responses associated with head injury, AD, alcohol use, thyroid disease, heart disease, and body mass index clustered in class A, while all responses associated with hypertension, Parkinson's disease, diabetes, and smoking clustered in class B. Within each class, responses were found to be organized by cell type (Figure 3 panel B).

3.3 Class A and B push a set of molecular pathways in opposite directions

Mitochondrial dysfunction [35, 36], endolysosomal dysfunction [37], loss of ribosome function [38] and programmed neuronal cell death [39] are well-known hallmarks of the AD brain. We observe that class A comorbidities robustly downregulate these pathways across multiple cell types, while class B phenotypes upregulate them (Figure 3 panels C and D).

Furthermore, we identify a convergent module of 17 genes downregulated by every class A comorbidity (Table 3).

The separation of comorbidities into class A or class B is not explained by brain versus non-brain or vascular versus non-vascular conditions. Instead, we propose that conditions separate into class A and class B based on whether the bioenergetic state of cells allow them to mount an adaptive stress response. In particular, non-lethal levels of mitochondrial stress are known to induce mitochondrial biogenesis and increase antioxidant defenses [40]. This program is energetically expensive, requiring heightened levels of translation and ribosomal biogenesis. Furthermore, mitochondrial biogenesis is only possible with sufficient metabolic resources, because the activation of AMPK in response to decreased ATP levels is known to

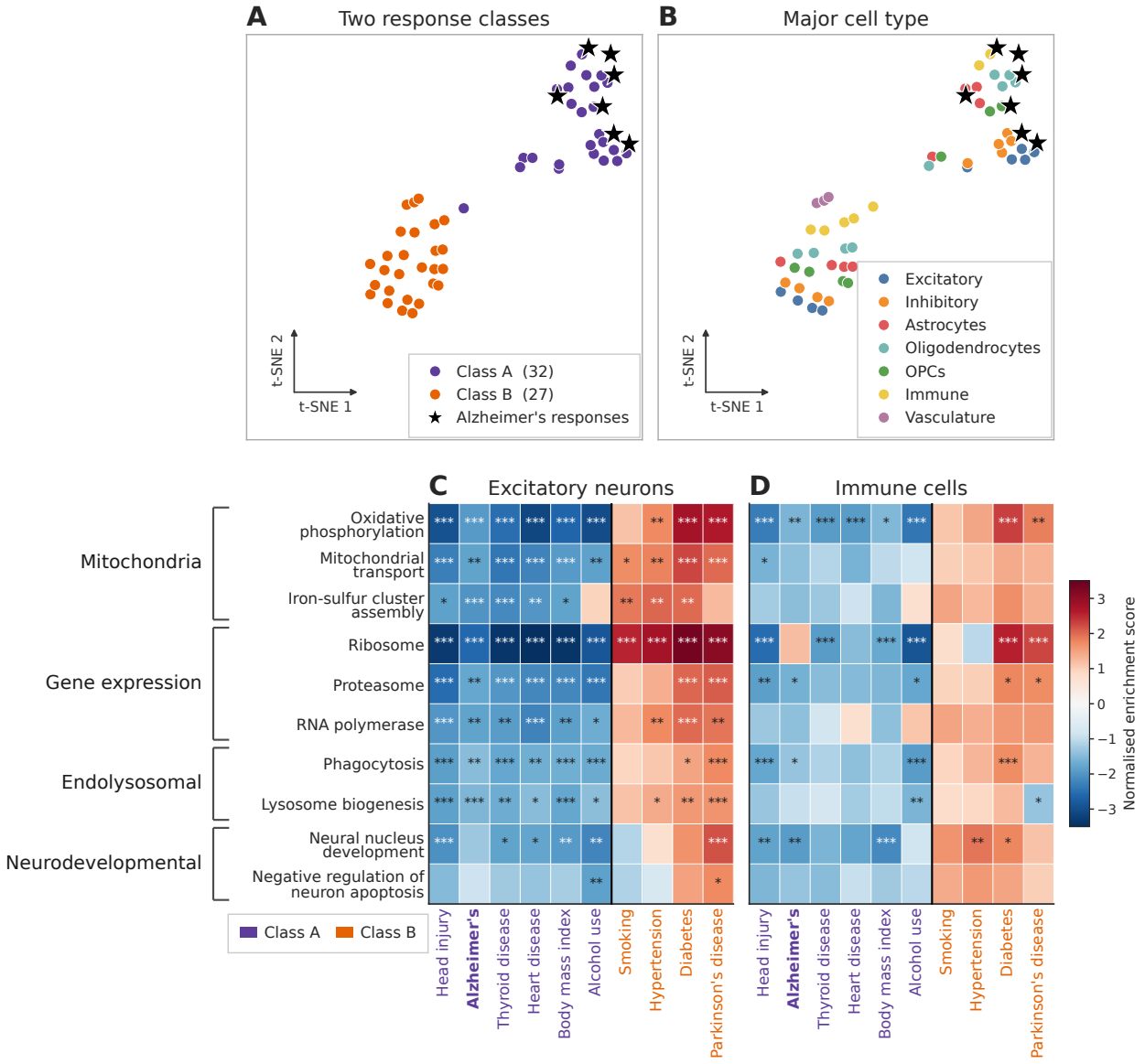

Figure 3: Transcriptional responses organize into two classes separated by phenotype. Class A responses were found to downregulate hallmark pathways that are also impaired in AD, while class B responses were found to upregulate those some pathways. **(A, B)** t-SNE embeddings of all 59 responses colored by **(A)** class and **(B)** cell type. **(C, D)** Ten GOBP and KEGG pathways corresponding to four major cellular processes that are regulated in different directions by class A and class B phenotypes in excitatory neurons **(C)** and immune cells **(D)**. $*\,p_{\text{adj}} < 0.05$, $**\,p_{\text{adj}} < 0.01$, $***\,p_{\text{adj}} < 0.001$.

suppress translational machinery [41].

Class A conditions directly decrease the metabolic resources available to cells. Heart disease [42] and hypothyroidism (the most common form of thyroid disease) [43] both cause brain hypoperfusion by reducing systemic blood flow. Similarly, a study with 44 Japanese patients found that traumatic head injury leading to neuropsychologic deficits induced chronic brain hypometabolism [44]. Alcohol use [45] and obesity [46] are also associated with neuronal energy compromise.

Meanwhile, class B conditions do not impair blood flow or deplete the metabolic resources of cells in the same manner. During hypertension, cerebral autoregulation counters hypoperfusion and ensures that sufficient blood reaches the brain [47]. In type 2 diabetes, hyperglycemia actually drives increased electron transport chain activity [48].

This suggests that an important axis determining the effect of comorbidities on the brain is whether a condition stresses cells while still leaving sufficient metabolic resources for the cell to mount an adaptive response, or whether it directly impacts bioenergetic availability and starves the cell of energy required for biosynthetic programs.

3.4 Thyroid disease

Surprisingly, thyroid disease produced a relatively strong AD-like response in brain cells. This was an interesting discovery because thyroid disease is a common and treatable endocrine condition with relatively little known about its connection to neurodegenerative disease compared to other comorbidities. Previous work has established a modest but significant increase in the prevalence of AD among patients with thyroid disease [18]. We posit that the similar transcriptional responses of thyroid disease and AD may be the result of hypothyroidism repressing cerebral blood flow [43], creating an energy-scarce state which downregulates mitochondrial and translational function.

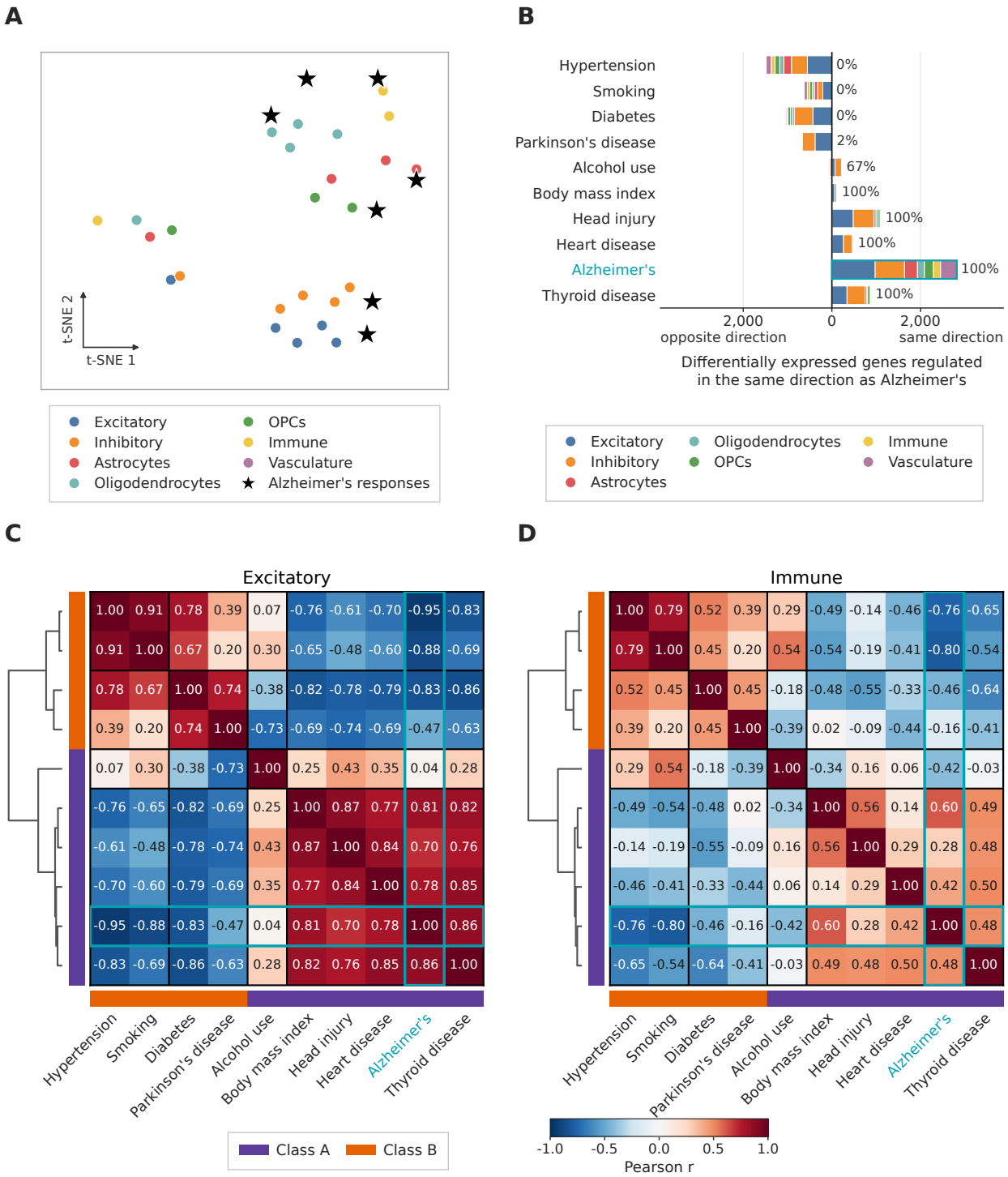

Figure 4: Class A comorbidities repress transcriptional programs known to be downregulated in AD, while class B comorbidities upregulate the same programs. **(A)** *t*-SNE embeddings of all 52 class A responses colored by cell type. **(B)** Percentage of DEGs shared with Alzheimer's disease, for each comorbidity. **(C, D)** Hierarchically clustered heatmap showing transcriptional similarity, quantified as Pearson correlation between gene expression vectors, of all conditions.

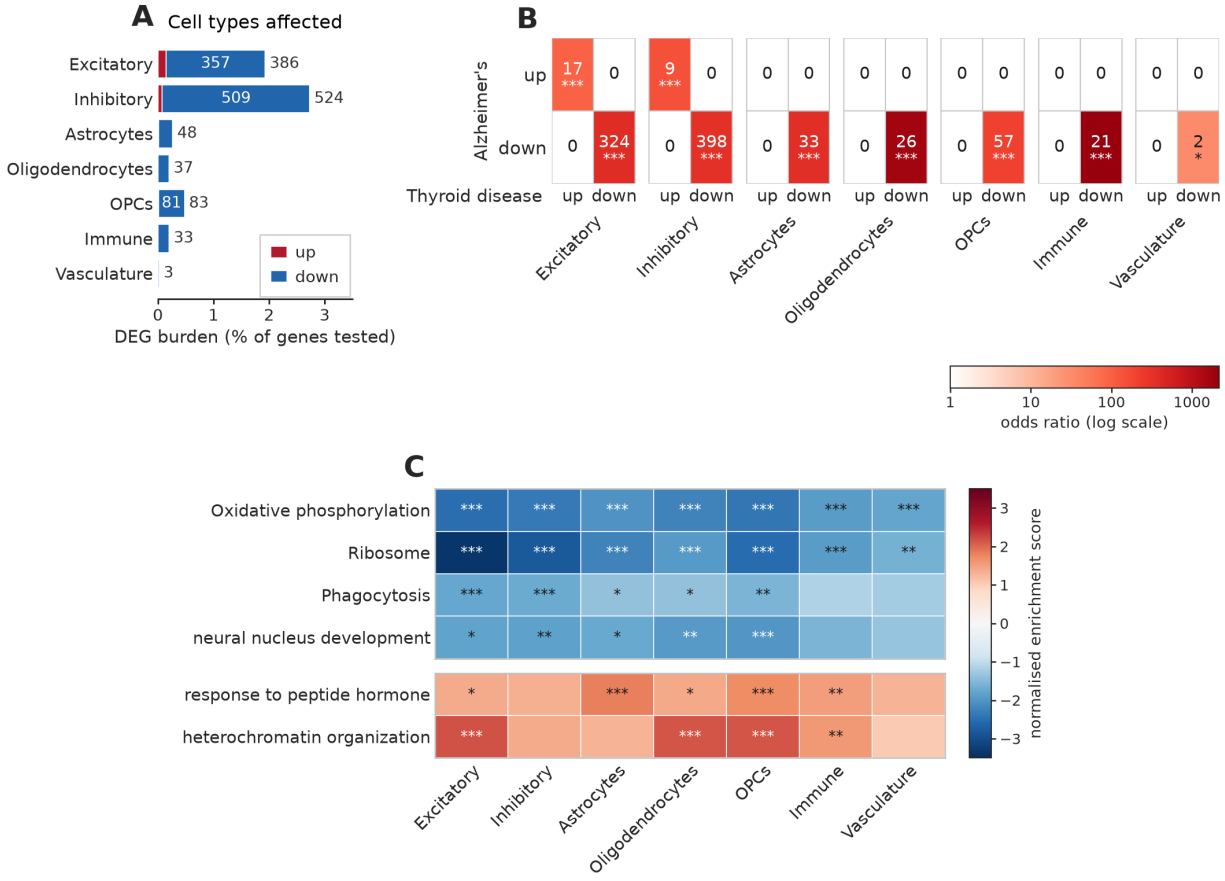

Figure 5: The transcriptional signature of thyroid disease mirrors that of AD extremely closely. **(A)** Stacked barplot showing DEG burden from thyroid disease across different cell types. **(B)** Faceted mirrored barplot showing enrichment of head-injury DEGs in AD DEGs. For each cell type, four one-sided Fisher exact tests were performed, and the odds ratio was calculated to quantify the enrichment of the thyroid disease down, thyroid disease up DEG list in the { AD down, AD up } DEG list. The number of shared DEGs is written within each bar. Cell types where zero DEGs were detected are indicated as not testable. **(C)** Heatmap showing upregulated and downregulated pathways in each cell type due to thyroid disease. $*\, p_{\text{adj}} < 0.05$, $**\, p_{\text{adj}} < 0.01$, $***\, p_{\text{adj}} < 0.001$.

4 Future work

Our analysis framework is dataset and phenotype agnostic, so the analysis completed here could easily be repeated for a larger dataset with more donors and more phenotypes. The Kellis lab has requested roughly 100 more clinical phenotype variables through the RADC Research Resource Sharing Hub; accessing this data would allow us to analyze many more lifestyle factors, personality traits, medication history data, etc. in the future. Analyzing the effects of statins or other lipid-lowering drugs on AD progression might allow us to understand how statins alter the cortical effects of hypertension.

We also plan on extending our framework to drug repurposing. Enrichment analyses between the genes we find convergent among our class A/B phenotypes and the genes which are targeted by a drug could reveal previously FDA-aproved drugs capable of preventing or treating AD.

5 Key Takeaways

We conducted the first single-cell resolution transcriptomic analysis investigating the responses of brain cells to a variety of AD comorbidities. We identified vulnerable cell types with high DEG burdens and discovered that clinically distinct phenotypes converge into two major classes of transcriptional response, and that all phenotypes within a class affect cortical transcriptional state in a similar way. Ultimately, by elucidating the molecular mechanisms which increase AD risk, this work sets the foundation for the development of preventative therapeutics for AD. Therapeutic agents which target multiple upstream AD risk factors stand a better chance of preventing AD than agents which only target downstream pathological factors which are likely the result of upstream dysfunction.

6 Acknowledgements

I would like to thank Dr. Shanshan Zhang for her invaluable guidance at every step of this project and Dr. Manolis Kellis for his advice, insights, and generosity. I thank Dr. Riley Mangan for developing the cell-projected phenotype (CPP) method and providing feedback and many aspects of my analysis. I would also like to thank my RSI tutor, Charles Xu, for providing valuable academic and personal advice, as well at the Center for Excellence in Education and MIT for supporting me this summer. Furthermore, thanks to my last-week TA Frederick Chen for his valuable feedback which helped me structure this paper. Finally, thanks to Mrs. Mary Waldman and Emmanuel Chang, M.D., Ph.D. for sponsoring me this summer and making this incredible opportunity possible.

Generative AI Statement

The generative Al tools ChatGPT, Claude, Claude Code, and Cursor were used to support this project by assisting with literature review and writing preliminary analysis code. These tools were used as research and computational aids only. All study design, data analysis, interpretation of results, and scientific conclusions were completed and verified by the author.

References

[1] R. J. Mangan, G. A. Bouland, T. Schubert, D. Anwer, J. Bai, G. Ekiz, N. Pigadas, A. Dattatri, A. Polster, A. Mahfouz, M. Reinders, and M. Kellis. Cell-projected Phenotypes Link Transcriptional and Phenotypic Heterogeneity in Alzheimer's Disease, Apr. 2026.

[2] 2025 Alzheimer's disease facts and figures. *Alzheimer's & Dementia*, 21(4):e70235, 2025. https://alz-journals.onlinelibrary.wiley.com/doi/abs/10.1002/alz.70235.

[3] K. B. Rajan, J. Weuve, L. L. Barnes, E. A. McAninch, R. S. Wilson, and D. A. Evans. Population estimate of people with clinical Alzheimer's disease and mild cognitive impairment in the United States (2020-2060). *Alzheimer's & Dementia: The Journal of the Alzheimer's Association*, 17(12):1966–1975, Dec. 2021.

[4] A. D. Korczyn. Why have we failed to cure Alzheimer's disease? *Journal of Alzheimer's Disease*, 29(2):275–282, 2012.

[5] J. L. Cummings, T. Morstorf, and K. Zhong. Alzheimer's disease drug-development pipeline: few candidates, frequent failures. *Alzheimer's Research & Therapy*, 6(4):37, 2014.

[6] C. H. van Dyck, C. J. Swanson, P. Aisen, R. J. Bateman, C. Chen, M. Gee, M. Kanekiyo, D. Li, L. Reyderman, S. Cohen, L. Froelich, S. Katayama, M. Sabbagh, B. Vellas, D. Watson, S. Dhadda, M. Irizarry, L. D. Kramer, and T. Iwatsubo. Lecanemab in early Alzheimer's disease. *New England Journal of Medicine*, 388(1):9–21, 2023.

[7] J. R. Sims, J. A. Zimmer, C. D. Evans, M. Lu, P. Ardayfio, J. Sparks, A. M. Wessels, S. Shcherbinin, H. Wang, E. S. Monkul Nery, E. C. Collins, P. Solomon, S. Salloway, L. G. Apostolova, O. Hansson, C. Ritchie, D. A. Brooks, M. Mintun, and D. M. Skovronsky. Donanemab in early symptomatic Alzheimer disease: The TRAILBLAZER-ALZ 2 randomized clinical trial. *JAMA*, 330(6):512–527, 2023.

[8] P. Hunter. The controversy around anti-amyloid antibodies for treating Alzheimer's disease. *EMBO Reports*, 25(12):5227–5231, Dec. 2024. https://doi.org/10.1038/s44319-024-00294-4.

[9] L. E. Stirland, R. Choate, P. P. Zanwar, P. Zhang, T. J. Watermeyer, M. Valletta, M. Torso, S. Tamburin, U. Saeed, G. R. Ridgway, S. Moukaled, J. B. Lusk, S. M. Loi, T. J. Littlejohns, E. Kuźma, S.-N. James, G. Grande, I. F. Foote, K. A. Q. Cousins,

J. Butler, A. AbuHamdia, T. J. Avelino-Silva, and V. Suryadevara. Multimorbidity in dementia: Current perspectives and future challenges. *Alzheimer's & Dementia: The Journal of the Alzheimer's Association*, 21(8):e70546, Aug. 2025.

[10] B. M. Tijms, E. M. Vromen, O. Mjaavatten, H. Holstege, L. M. Reus, S. van der Lee, K. E. J. Wesenhagen, L. Lorenzini, L. Vermunt, V. Venkatraghavan, N. Tesi, J. Tomassen, A. den Braber, J. Goossens, E. Vanmechelen, F. Barkhof, Y. A. L. Pijnenburg, W. M. van der Flier, C. E. Teunissen, F. S. Berven, and P. J. Visser. Cerebrospinal fluid proteomics in patients with Alzheimer's disease reveals five molecular subtypes with distinct genetic risk profiles. *Nature Aging*, 4(1):33–47, Jan. 2024.

[11] A. Ott, R. P. Stolk, F. van Harskamp, H. A. Pols, A. Hofman, and M. M. Breteler. Diabetes mellitus and the risk of dementia: The Rotterdam Study. *Neurology*, 53(9):1937–1942, Dec. 1999.

[12] Z. Arvanitakis, R. S. Wilson, J. L. Bienias, D. A. Evans, and D. A. Bennett. Diabetes mellitus and risk of Alzheimer disease and decline in cognitive function. *Archives of Neurology*, 61(5):661–666, 2004.

[13] M. G. Marmot, S. Stansfeld, C. Patel, F. North, J. Head, I. White, E. Brunner, A. Feeney, M. G. Marmot, and G. D. Smith. Health inequalities among British civil servants: the Whitehall II study. *The Lancet*, 337(8754):1387–1393, June 1991. https://www.sciencedirect.com/science/article/pii/014067369193068K.

[14] J. G. Abell, M. Kivimäki, A. Dugravot, A. G. Tabak, A. Fayosse, M. Shipley, S. Sabia, and A. Singh-Manoux. Association between systolic blood pressure and dementia in the Whitehall II cohort study: role of age, duration, and threshold used to define hypertension. *European Heart Journal*, 39(33):3119–3125, Sept. 2018.

[15] M. Kivipelto, T. Ngandu, L. Fratiglioni, M. Viitanen, I. Kåreholt, B. Winblad, E.-L. Helkala, J. Tuomilehto, H. Soininen, and A. Nissinen. Obesity and vascular risk factors at midlife and the risk of dementia and Alzheimer disease. *Archives of Neurology*, 62(10):1556–1560, Oct. 2005.

[16] S. Alford, D. Patel, N. Perakakis, and C. S. Mantzoros. Obesity as a risk factor for Alzheimer's disease: weighing the evidence. *Obesity Reviews*, 19(2):269–280, 2018. _eprint: https://onlinelibrary.wiley.com/doi/pdf/10.1111/obr.12629, https://onlinelibrary.wiley.com/doi/abs/10.1111/obr.12629.

[17] B. L. Plassman, R. J. Havlik, D. C. Steffens, M. J. Helms, T. N. Newman, D. Drosdick, C. Phillips, B. A. Gau, K. A. Welsh-Bohmer, J. R. Burke, J. M. Guralnik, and J. C. Breitner. Documented head injury in early adulthood and risk of Alzheimer's disease and other dementias. *Neurology*, 55(8):1158–1166, Oct. 2000.

[18] J. H. Kim, H. S. Lee, Y. H. Kim, M. J. Kwon, J.-H. Kim, C. Y. Min, D. M. Yoo, and H. G. Choi. The Association Between Thyroid Diseases and Alzheimer's Disease in a National Health Screening Cohort in Korea. *Frontiers in Endocrinology*, 13, Mar. 2022. Publisher: Frontiers, https://www.frontiersin.org/journals/endocrinology/articles/10.3389/fendo.2022.815063/full.

[19] P. Zhang, H. J. Edenberg, J. Nurnberger, D. Lai, F. Cheng, and Y. Liu. Alcohol use disorder is associated with higher risks of Alzheimer's and Parkinson's diseases: A study of US insurance claims data. *Alzheimer's & Dementia : Diagnosis, Assessment & Disease Monitoring*, 14(1):e12370, Nov. 2022. https://pmc.ncbi.nlm.nih.gov/articles/PMC9677510/.

[20] A. Ott, A. J. Slooter, A. Hofman, F. van Harskamp, J. C. Witteman, C. Van Broeckhoven, C. M. van Duijn, and M. M. Breteler. Smoking and risk of dementia and Alzheimer's disease in a population-based cohort study: the Rotterdam Study. *Lancet*, 351(9119):1840–1843, June 1998. Place: London, England.

[21] T.-Y. Chang, C.-P. Yang, Y.-H. Chen, C.-H. Lin, and M.-H. Chang. Age-Stratified Risk of Dementia in Parkinson's Disease: A Nationwide, Population-Based, Retrospective Cohort Study in Taiwan. *Frontiers in Neurology*, 12, Dec. 2021. Publisher: Frontiers, https://www.frontiersin.org/journals/neurology/articles/10.3389/fneur.2021.748096/full.

[22] G. Livingston, J. Huntley, A. Sommerlad, D. Ames, C. Ballard, S. Banerjee, C. Brayne, A. Burns, J. Cohen-Mansfield, C. Cooper, S. G. Costafreda, A. Dias, N. Fox, L. N. Gitlin, R. Howard, H. C. Kales, M. Kivimäki, E. B. Larson, A. Ogunniyi, V. Orgeta, K. Ritchie, K. Rockwood, E. L. Sampson, Q. Samus, L. S. Schneider, G. Selbæk, L. Teri, and N. Mukadam. Dementia prevention, intervention, and care: 2020 report of the Lancet Commission. *The Lancet*, 396(10248):413–446, Aug. 2020. Publisher: Elsevier, https://www.thelancet.com/article/S0140-6736(20)30367-6/fulltext.

[23] A. P. Pérez-González, A. L. García-Kroepfly, K. A. Pérez-Fuentes, R. I. García-Reyes, F. F. Solis-Roldan, J. A. Alba-González, E. Hernández-Lemus, and G. de Anda-Jáuregui. The ROSMAP project: aging and neurodegenerative diseases through omic sciences. *Frontiers in Neuroinformatics*, 18:1443865, Sept. 2024. https://pmc.ncbi.nlm.nih.gov/articles/PMC11439699/.

[24] D. Jovic, X. Liang, H. Zeng, L. Lin, F. Xu, and Y. Luo. Single-cell RNA sequencing technologies and applications: A brief overview. *Clinical and Translational Medicine*, 12(3):e694, Mar. 2022. https://pmc.ncbi.nlm.nih.gov/articles/PMC8964935/.

[25] R. V. Grindberg, J. L. Yee-Greenbaum, M. J. McConnell, M. Novotny, A. L. O'Shaughnessy, G. M. Lambert, M. J. Araúzo-Bravo, J. Lee, M. Fishman, G. E. Robbins, X. Lin, P. Venepally, J. H. Badger, D. W. Galbraith, F. H. Gage, and R. S. Lasken. RNA-sequencing from single nuclei. *Proceedings of the National Academy of Sciences of the United States of America*, 110(49):19802–19807, Dec. 2013.

[26] H. Mathys, Z. Peng, C. A. Boix, M. B. Victor, N. Leary, S. Babu, G. Abdelhady, X. Jiang, A. P. Ng, K. Ghafari, A. K. Kunisky, J. Mantero, K. Galani, V. N. Lohia, G. E. Fortier, Y. Lotfi, J. Ivey, H. P. Brown, P. R. Patel, N. Chakraborty, J. I. Beaudway, E. J. Imhoff, C. F. Keeler, M. M. McChesney, H. H. Patel, S. P. Patel, M. T. Thai, D. A. Bennett, M. Kellis, and L.-H. Tsai. Single-cell atlas reveals correlates of high cognitive function, dementia, and resilience to Alzheimer's disease pathology. *Cell*, 186(20):4365–4385.e27, 2023.

[27] A. Subramanian, P. Tamayo, V. K. Mootha, S. Mukherjee, B. L. Ebert, M. A. Gillette, A. Paulovich, S. L. Pomeroy, T. R. Golub, E. S. Lander, and J. P. Mesirov. Gene set enrichment analysis: a knowledge-based approach for interpreting genome-wide expression profiles. *Proceedings of the National Academy of Sciences of the United States of America*, 102(43):15545–15550, Oct. 2005.

[28] G. Korotkevich, V. Sukhov, N. Budin, B. Shpak, M. N. Artyomov, and A. Sergushichev. Fast gene set enrichment analysis, Feb. 2021. Pages: 060012 Section: New Results.

[29] M. Zhao, H. Jia, N. Li, M. Zhao, H. Jia, and N. Li. Astrocyte–Neuron Crosstalk in Hypertension: Mechanisms and Therapeutic Significance. *Reviews in Cardiovascular Medicine*, 27(4), Apr. 2026. Publisher: IMR Press, https://www.imrpress.com/journal/RCM/27/4/10.31083/RCM47764.

[30] S. Schreiber, P. Arndt, L. Morton, A. P. Garza, P. Müller, K. Neumann, H. Mattern, M. Dörner, J. Bernal, S. Vielhaber, S. G. Meuth, I. R. Dunay, A. Dityatev, and S. Henneicke. Immune system activation and cognitive impairment in arterial hypertension. *American Journal of Physiology-Cell Physiology*, 327(6):C1577–C1590, 2024. PMID: 39495252, https://doi.org/10.1152/ajpcell.00219.2024.

[31] L.-P. Wang, J. Geng, C. Liu, Y. Wang, Z. Zhang, and G.-Y. Yang. Diabetes Mellitus-Related Neurobehavioral Deficits in Mice Are Associated With Oligodendrocyte Precursor Cell Dysfunction. *Frontiers in Aging Neuroscience*, 14, May 2022. Publisher: Frontiers, https://www.frontiersin.org/journals/aging-neuroscience/articles/10.3389/fnagi.2022.846739/full.

[32] E. K. Erickson, S. P. Farris, Y. A. Blednov, R. D. Mayfield, and R. A. Harris. Astrocyte-Specific Transcriptome Responses to Chronic Ethanol Consumption. *The pharmacogenomics journal*, 18(4):578–589, July 2018. https://pmc.ncbi.nlm.nih.gov/articles/PMC6033697/.

[33] F. Guo, Y.-F. Zhang, K. Liu, X. Huang, R.-X. Li, S.-Y. Wang, F. Wang, L. Xiao, F. Mei, and T. Li. Chronic Exposure to Alcohol Inhibits New Myelin Generation in Adult Mouse Brain. *Frontiers in Cellular Neuroscience*, 15, Aug. 2021. Publisher: Frontiers, https://www.frontiersin.org/journals/cellular-neuroscience/articles/10.3389/fncel.2021.732602/full.

[34] F.-L. Zhang, A.-Y. Li, Y.-L. Niu, K. Zhang, M.-H. Zhao, J.-J. Huang, and W. Shen. Identification of biomarkers in Parkinson's disease by comparative transcriptome analysis and WGCNA highlights the role of oligodendrocyte precursor cells. *Frontiers in Aging Neuroscience*, 16, Nov. 2024. Publisher: Frontiers, https://www.frontiersin.org/journals/aging-neuroscience/articles/10.3389/fnagi.2024.1485722/full.

[35] K. Chandrasekaran, K. Hatanpää, D. R. Brady, and S. I. Rapoport. Evidence for physiological down-regulation of brain oxidative phosphorylation in Alzheimer's disease. *Experimental Neurology*, 142(1):80–88, Nov. 1996.

[36] P. J. Flannery and E. Trushina. Mitochondrial Dynamics and Transport in Alzheimer's Disease. *Molecular and cellular neurosciences*, 98:109–120, July 2019. https://pmc.ncbi.nlm.nih.gov/articles/PMC6614006/.

[37] L. S. Whyte, A. A. Lau, K. M. Hemsley, J. J. Hopwood, and T. J. Sargeant. Endo-lysosomal and autophagic dysfunction: a driving factor in Alzheimer's disease? *Journal of Neurochemistry*, 140(5):703–717, 2017. https://onlinelibrary.wiley.com/doi/abs/10.1111/jnc.13935.

[38] Q. Ding, W. R. Markesbery, Q. Chen, F. Li, and J. N. Keller. Ribosome Dysfunction Is an Early Event in Alzheimer's Disease. *Journal of Neuroscience*, 25(40):9171–9175, Oct. 2005. Publisher: Society for Neuroscience Section: Brief Communications, https://www.jneurosci.org/content/25/40/9171.

[39] D. Moujalled, A. Strasser, and J. R. Liddell. Molecular mechanisms of cell death in neurological diseases. *Cell Death & Differentiation*, 28(7):2029–2044, July 2021. Publisher: Nature Publishing Group, https://www.nature.com/articles/s41418-021-00814-y.

[40] J. Yun and T. Finkel. Mitohormesis. *Cell Metabolism*, 19(5):757–766, May 2014.

[41] Y.-J. Liu and Y. Chern. Contribution of Energy Dysfunction to Impaired Protein Translation in Neurodegenerative Diseases. *Frontiers in Cellular Neuroscience*, 15:668500, July 2021. https://pmc.ncbi.nlm.nih.gov/articles/PMC8355359/.

[42] A. Ovsenik, M. Podbregar, and A. Fabjan. Cerebral blood flow impairment and cognitive decline in heart failure. *Brain and Behavior*, 11(6):e02176, June 2021.

[43] E. L. Constant, A. G. de Volder, A. Ivanoiu, A. Bol, D. Labar, A. Seghers, G. Cosnard, J. Melin, and C. Daumerie. Cerebral blood flow and glucose metabolism in hypothyroidism: a positron emission tomography study. *The Journal of Clinical Endocrinology and Metabolism*, 86(8):3864–3870, Aug. 2001.

[44] T. Nakashima, N. Nakayama, K. Miwa, A. Okumura, A. Soeda, and T. Iwama. Focal brain glucose hypometabolism in patients with neuropsychologic deficits after diffuse axonal injury. *AJNR. American journal of neuroradiology*, 28(2):236–242, Feb. 2007.

[45] R. F. Butterworth, J. J. Kril, and C. G. Harper. Thiamine-dependent enzyme changes in the brains of alcoholics: relationship to the Wernicke-Korsakoff syndrome. *Alcoholism, Clinical and Experimental Research*, 17(5):1084–1088, Oct. 1993.

[46] K. C. Willeumier, D. V. Taylor, and D. G. Amen. Elevated BMI Is Associated With Decreased Blood Flow in the Prefrontal Cortex Using SPECT Imaging in Healthy Adults. *Obesity (Silver Spring, Md.)*, 19(5):1095–1097, May 2011. https://pmc.ncbi.nlm.nih.gov/articles/PMC3125099/.

[47] S. Strandgaard and O. B. Paulson. Cerebral autoregulation. *Stroke*, 15(3):413–416, 1984. https://www.ahajournals.org/doi/abs/10.1161/01.STR.15.3.413.

[48] T. Nishikawa, D. Edelstein, X. L. Du, S. Yamagishi, T. Matsumura, Y. Kaneda, M. A. Yorek, D. Beebe, P. J. Oates, H. P. Hammes, I. Giardino, and M. Brownlee. Normalizing mitochondrial superoxide production blocks three pathways of hyperglycaemic damage. *Nature*, 404(6779):787–790, Apr. 2000.

A Appendix

Comorbidity	Class	Donors		DEGs by cell type							Total
		Low	High	Exc	Inh	Ast	Oli	OPC	Imm	Vas	
Head injury	A	23–37	9–14	992	1,266	137	259	214	68	0	2,936
Alzheimer's disease	A	75–92	85–97	976	663	291	159	200	164	366	2,819
Hypertension	B	38–43	47–52	651	415	327	129	231	200	211	2,164
Parkinson's disease	B	99–108	11–13	1,013	674	38	87	232	21	0	2,065
Diabetes	B	91–101	18–24	510	604	44	124	167	72	45	1,566
Alcohol use	A	23–41	47–54	311	497	207	37	142	67	1	1,262
Thyroid disease	A	62–81	21–23	386	524	48	37	83	33	3	1,114
Smoking	B	57–68	42–45	243	146	95	49	80	78	93	784
Heart disease	A	37–45	29–38	312	240	45	11	0	1	0	609
Body mass index	A	60–69	52–60	71	41	0	10	0	7	7	136
Total				5,465	5,070	1,232	902	1,349	711	726	15,455

Table 2: Number of DEG calls and number of donors for each of the nine comorbidity comparisons plus the Alzheimer's disease comparison. The donor column show the minimum and maximum number of donors across the seven cell type comparisons, reflecting the exclusion of donors with fewer than ten cells. DEGs were called at $p_{\text{adj}} < 0.05$ and $|\log_2 \text{FC}| > 0.5$.

Table 3: The convergent module of 17 genes, grouped by function. Values are $\log_2$ fold changes in the AD reference contrast across seven major cell types.

Gene	Function	Exc	Inh	Ast	Oli	OPC	Imm	Vas
Protein synthesis								
RPL41	Large ribosomal subunit	−1.54	−1.50	−0.77	−0.44	−0.57	−0.09	−0.32
SRP14	Signal recognition particle	−0.78	−0.70	−0.34	−0.66	−0.27	−1.05	−0.36
RPS4X	Small ribosomal subunit	−1.11	−1.20	−0.74	−0.31	−0.68	−0.07	−0.54
RPS7	Small ribosomal subunit	−1.14	−1.18	−0.57	−0.20	−0.55	−0.01	−0.12
FAU	Ubiquitin–ribosomal protein	−0.98	−1.01	−0.60	−0.23	−0.23	+0.08	−0.25
Cytoskeleton								
TMSB10	Actin sequestration	−0.66	−0.95	−1.23	−1.35	−1.15	+0.15	+0.26
TUBB2A	Beta-tubulin	−1.14	−1.09	−0.84	−2.20	−1.18	−2.27	−1.43
STMN1	Microtubule destabilization	−0.63	−0.71	−1.19	−0.25	−0.67	−1.50	−1.39
Vesicle traffic and acidification								
RAB3A	Synaptic vesicle release	−0.73	−0.77	−1.38	−1.63	−1.23	−1.90	−1.99
ATP6V1F	V-ATPase acidification	−0.77	−0.84	−0.87	−0.72	−0.52	−0.67	−0.74
ARF5	Vesicle trafficking	−1.12	−1.20	−0.35	−0.55	−0.43	−0.33	−0.81
Mitochondrial transport								
SLC25A5	ADP/ATP transport	−1.07	−1.13	−0.78	−0.42	−0.59	−0.57	−0.38
PRELID1	Phospholipid transfer	−0.95	−0.80	−0.45	−0.31	−0.36	−0.42	−0.28
Neuronal signaling								
GNG3	G-protein gamma subunit	−0.80	−0.77	−1.56	−1.97	−0.32	−2.21	−1.53
BEX3	p75NTR-associated protein	−1.09	−1.15	−0.93	−0.81	−0.61	−1.92	−0.98
Redox								
GSTP1	Glutathione transferase	−0.70	−0.80	−0.39	−0.34	−0.39	−0.19	−0.06
SELENOM	ER redox protein	−0.98	−0.94	−0.44	−0.31	−0.30	−0.63	−0.47